EFFECT OF ION CYCLOTRON HEATING ON FAST ION TRANSPORT AND PLASMA ROTATION IN TOKAMAKS

by
V.S. Chan, S.C. Chiu, and Y.A. Omelchenko

Presented at
the American Physical Society
Division of Plasma Physics Meeting
Quebec City, Canada

The authors acknowledge many useful discussions with
F.W. Perkins and the use of the ORBIT code from R.B. White

October 23–27, 2000

GENERAL ATOMICS

MOTIVATION

- Recently, Alcator C–Mod has discovered that plasmas with fast wave minority heating can develop an appreciable co-current toroidal rotation in the vicinity of the magnetic axis, even though the heating method provides negligible angular momentum [Rice, J.E., et al., Nucl. Fusion 38 (1998) 75; Rice, J.E., et al., Nucl. Fusion 39 (1999) 1175]

- A mechanism proposed by Perkins and White (invited talk DPP00) and demonstrated using Monte-Carlo orbit simulations showed a number of relevant features
  - No angular momentum input from the energetic minority ions
  - Using a non-slip boundary condition at the plasma edge, co-rotation is computed with low-field side (LFS) ion cyclotron resonance heating
  - The angular rotation scales with stored energy

PRESENT STUDY

- **Issues**
  - An explanation of a net co-current torque with LFS resonance and a net counter-current torque with HFS resonance in Perkin's model
  - The model predicts counter-current toroidal rotation when the resonance is on the high field side (HFS); recent C–Mod experiment (2000) did not see this

- **Approach: An rf diffusion operator is added to the Monte-Carlo orbit code (ORBIT originally developed by R.B. White)**
  - Stochastic "kick" in perpendicular energy consistent with quasi-linear diffusion
  - Wave zone modeled after full wave code; electric field E_+ consistent with code
  - Finite $N_{||}$ (symmetric or asymmetric spectrum) and Doppler resonance included (Omelchenko DPP99, see detailed description of code later in this poster)

KEY RESULTS

- A more realistic model of rf heating can produce a toroidal drift in the velocity distribution for minority species with symmetric wavenumber spectrum i.e. can induce angular momentum torque (consequence of finite orbit). However, it is small for the cases studied

- Two cases were studied
  - Case 1: RF created initial energetic ions, magnetic and frictional torque allowed to balance
    - ★ Co-current rotation with LFS resonance heating
      - ◊ Due to favorable frictional torque of energetic, co-passing minority ions
    - ★ Counter-current rotation with HFS resonance heating
      - ◊ Due to favorable frictional torque of barely-untrapped, counter-passing minority ions
  - Case 2: Using a model for a steady-state minority ion source, similar features to Case 1 are reproduced

A MORE REALISTIC RF HEATING MODEL CAN PRODUCE AN ASYMMETRIC VELOCITY DISTRIBUTION

- RF heating increases the minority ion orbit from thin to fat bananaution
  - Constant of motion: $\Psi_* = \Psi - I\, v_{||}/\Omega$
  - Collisions break orbit: $v_{||}$ (co-passing) > $v_{||}$ (counter-passing)

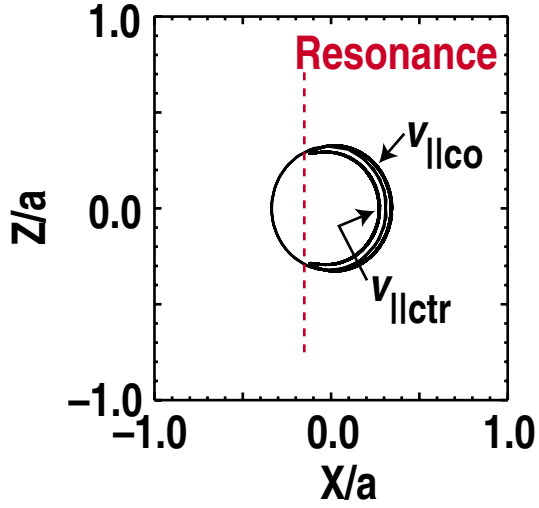

- The spatial distribution of fast ions peaks near the resonance

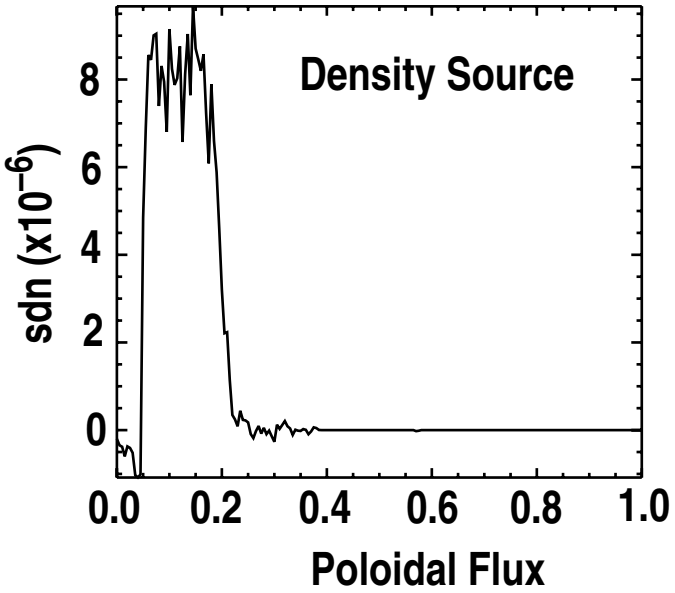

- Resultant distribution is asymmetric in $v_{||}$ with net momentum in the co-direction

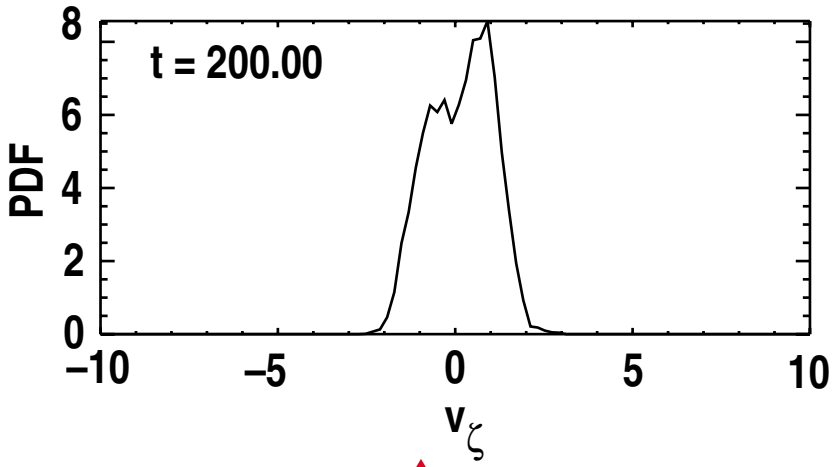

GENERAL ATOMICS

CASE 1: RF CREATED INITIAL ENERGETIC IONS, MAGNETIC AND FRICTIONAL TORQUE ALLOWED TO BALANCE

- Collisions scatter energetic particles inward and outward creating radial currents

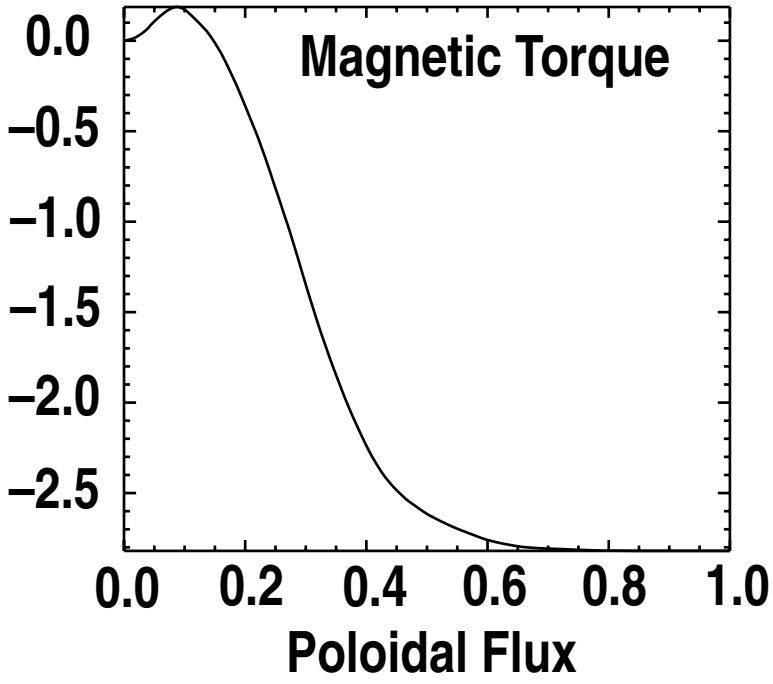

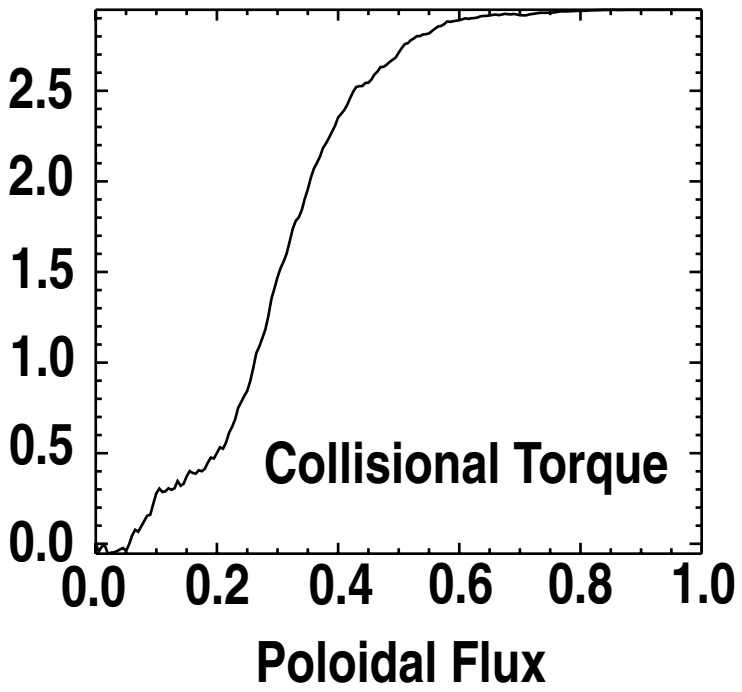

- J_{bulk}xB torque on the bulk due to return current in response to minority ions moving in (out): $J_{minority}$ out (in) $\Rightarrow$ J_{bulk}xB counter- (co-)
- Frictional torque on bulk exerted by minority ions due to combination of VxB and non-uniform radial distribution of co- and counter-passing ions

LOW FIELD SIDE RESONANCE PRODUCES CO-CURRENT ROTATION

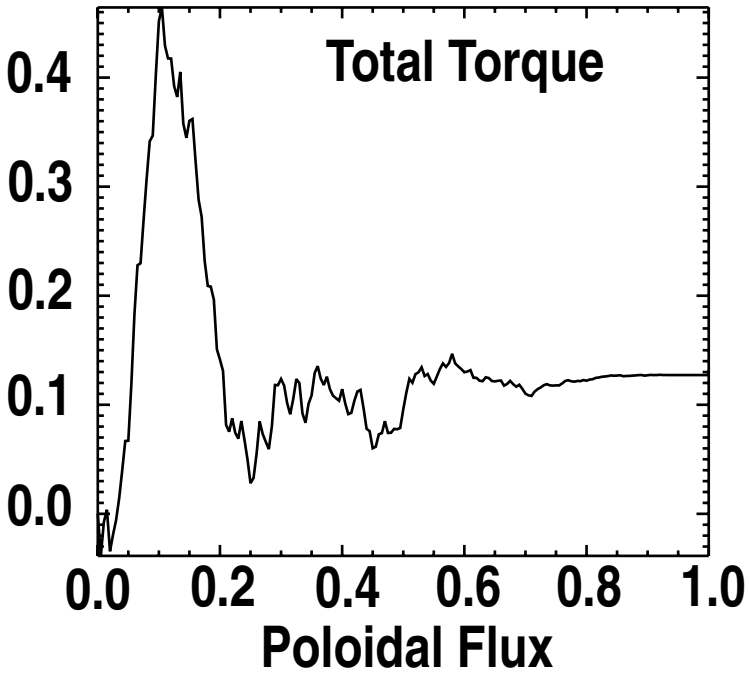

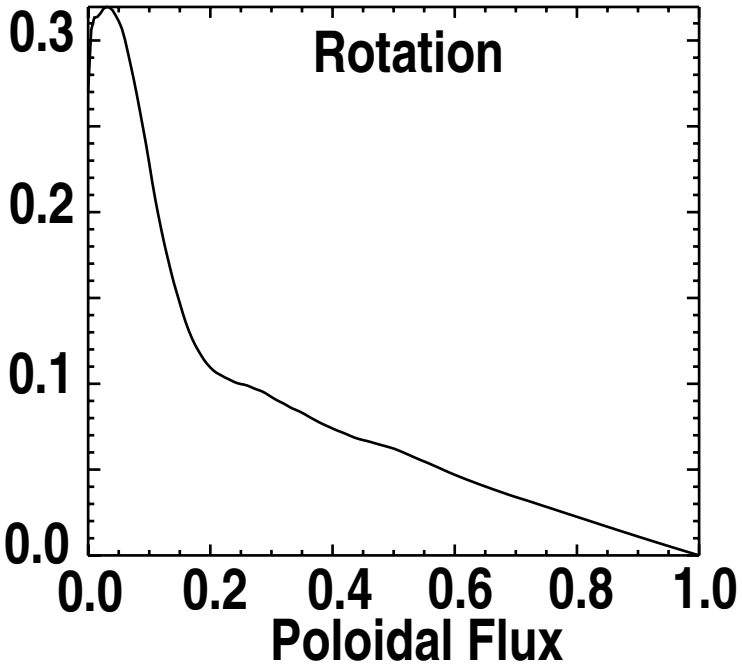

- Sum of JxB and frictional torque gives a net positive torque near the magnetic axis

- Balancing torque against angular momentum diffusion ($\tau_E = \tau_M$) and using non-slip boundary condition, co-rotation profile is obtained

POSITIVE FRICTIONAL TORQUE NEAR THE AXIS FOR LFS IS DUE TO MORE CO-PASSING IONS

- VxB force on minority ions inside resonance is counter-direction ⇒ frictional force on bulk is negative, cannot explain result

- LFS resonance (with $N_{||} = 0$) heats deeply trapped particles (not easily detrapped by coilisions). From finite drift orbit analysis (Chiu DPP99, see details below), particles scattered inwards can either remain trapped or become co-passing ⇒ co-current frictional torque is favored

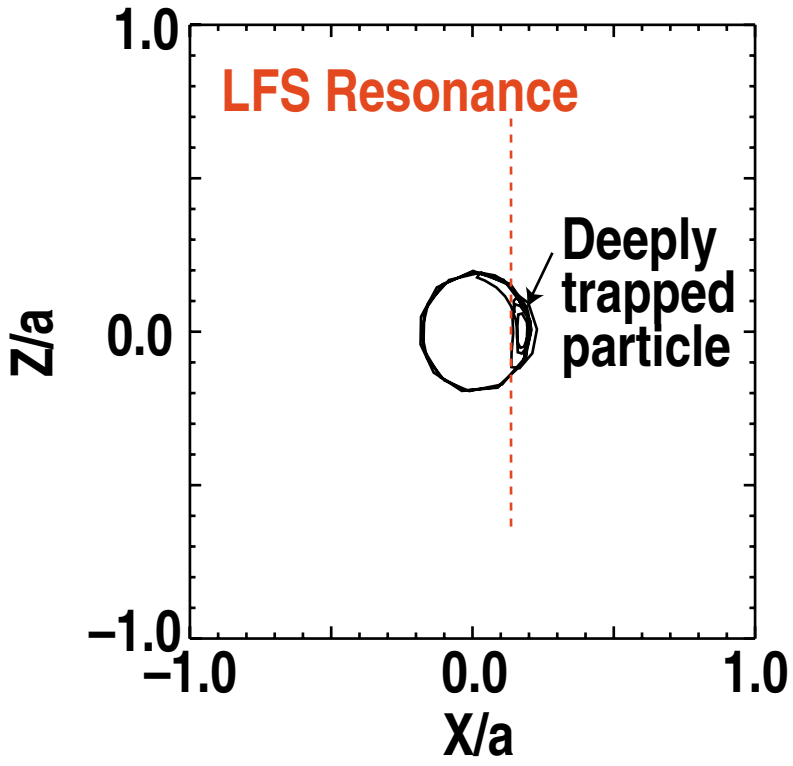

- An orbit illustrating this process is shown here

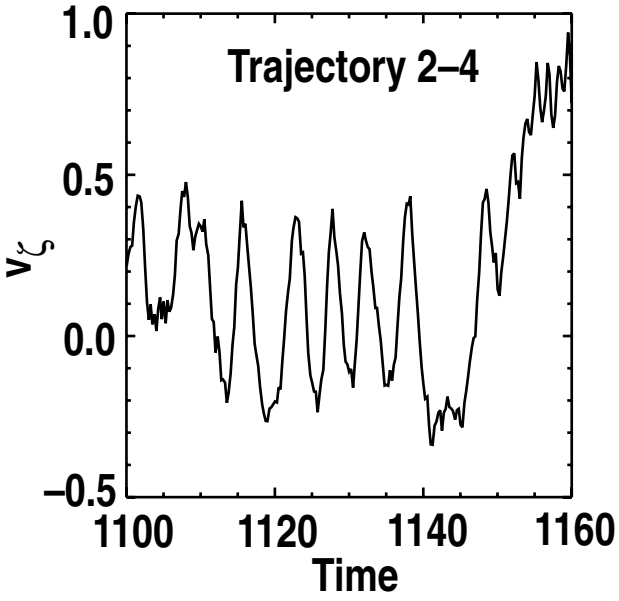

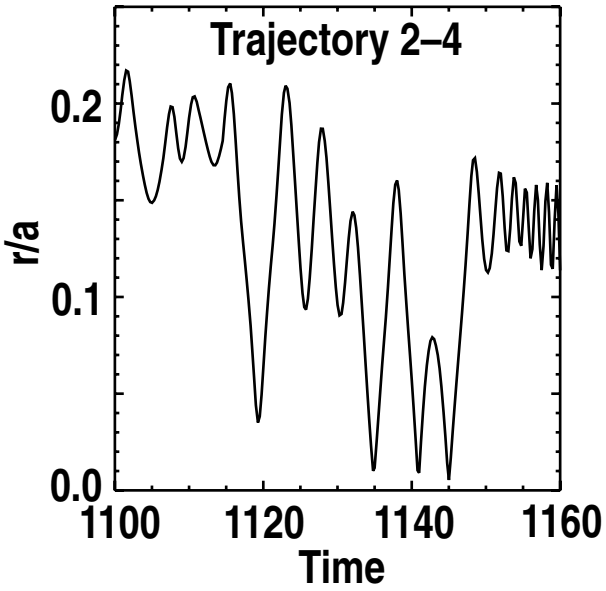

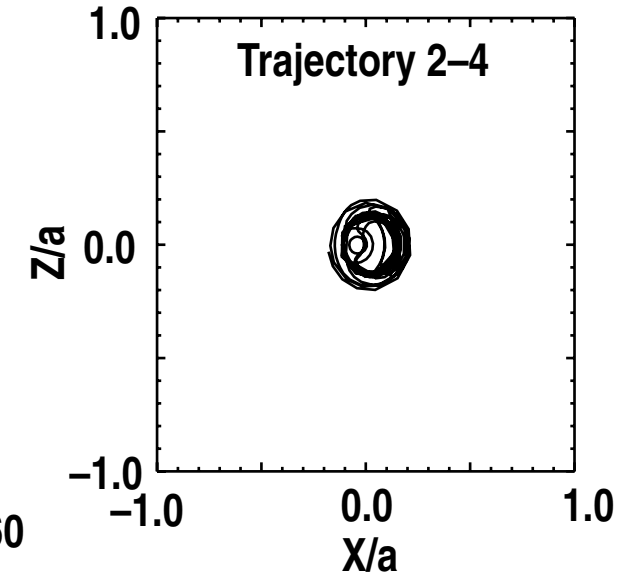

- Toroidal velocity becomes positive with time ⇒ co-passing
- Radius moves inward on average
- Cross section
  - ★ Fat banana orbit becomes co-passing orbit

HIGH FIELD SIDE RESONANCE PRODUCES COUNTER-CURRENT ROTATION

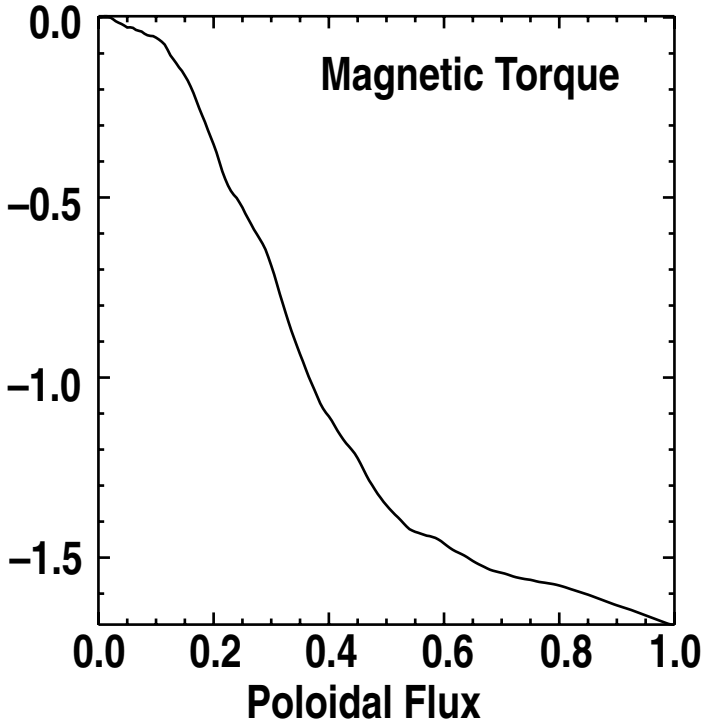

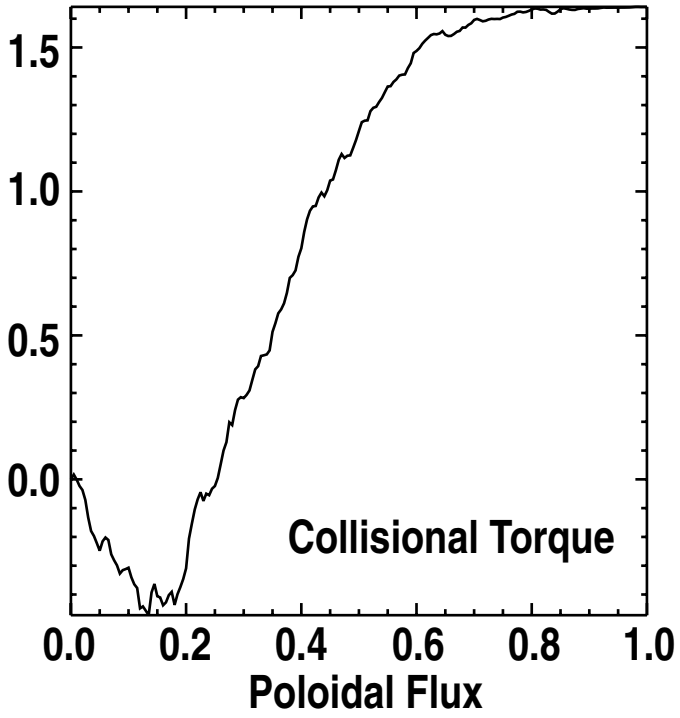

- J_{bulk}xB torque is similar to LFS $\Rightarrow$ both due to collisional scattering of resonance ions inwards and outwards
- Frictional torque clearly negative near the axis

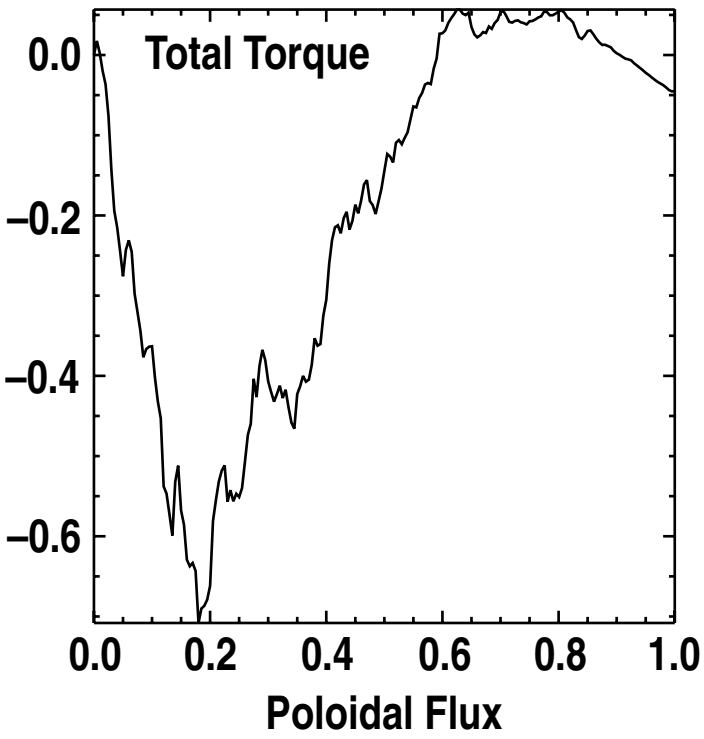

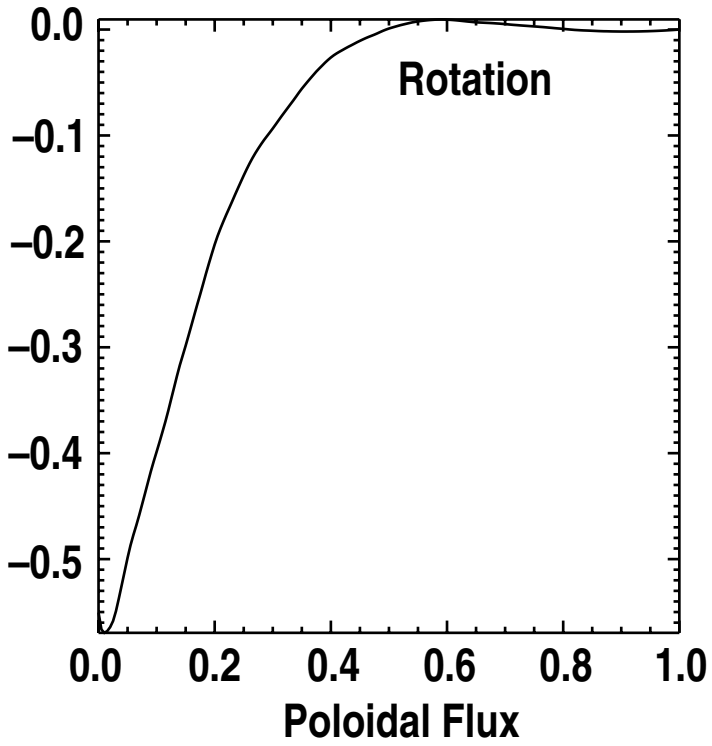

- Sum of JxB and frictional torque gives negative torque near the center (frictional torque larger)

- Rotation is in the counter direction

NEGATIVE FRICTIONAL TORQUE NEAR THE AXIS FOR HFS IS DUE TO MORE COUNTER-PASSING IONS

- The VxB frictional torque exerted on the bulk is largely cancelled by $J_{bulk}xB$ (in zero banana width approximation, they exactly cancel)
- HFS resonance heats barely trapped particles (easily detrapped). Because of finite orbit width, counter-passing particles moved inside and co-passing particles moved outside $\Rightarrow$ negative frictional torque inside

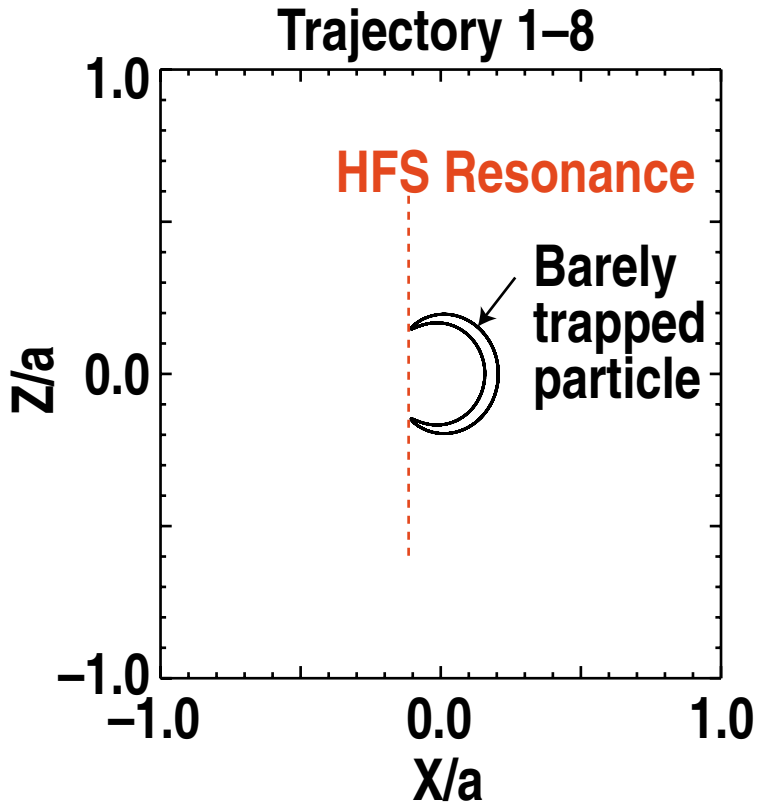

- An orbit illustrating this process is shown here

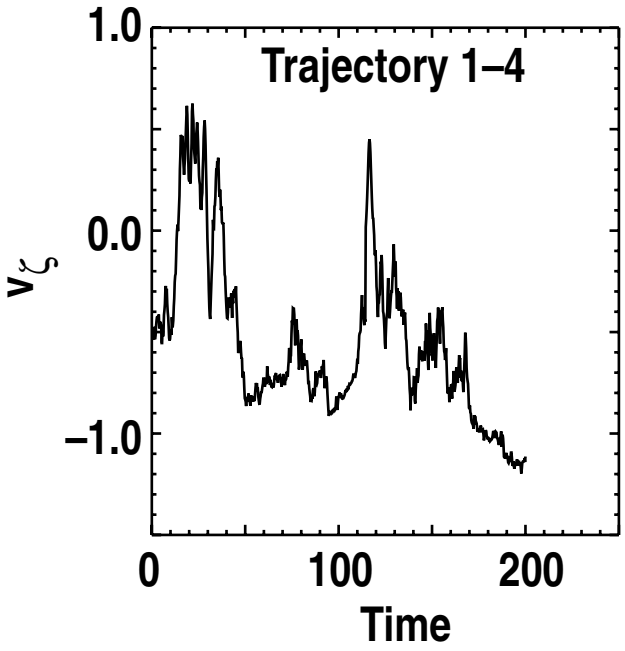

– Toroidal velocity becomes negative with time

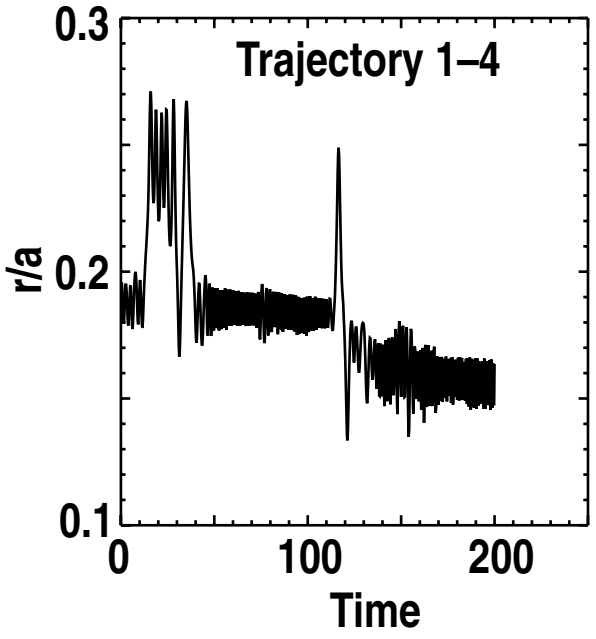

– Radius decreases with time on average

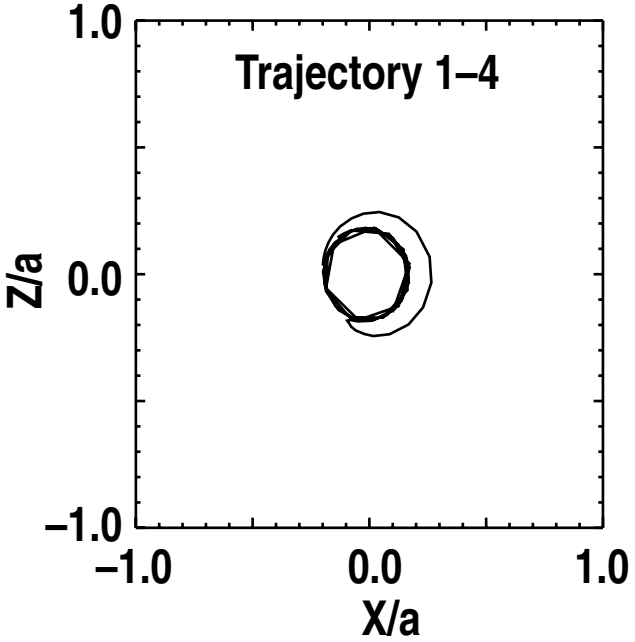

– Cross section

★ Barely trapped particle becomes counter-passing

ANALYSIS OF ORBITS NEAR THE AXIS

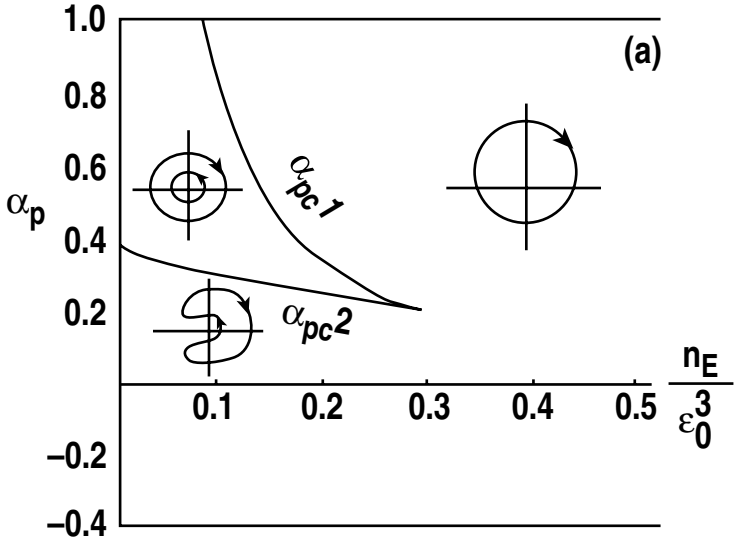

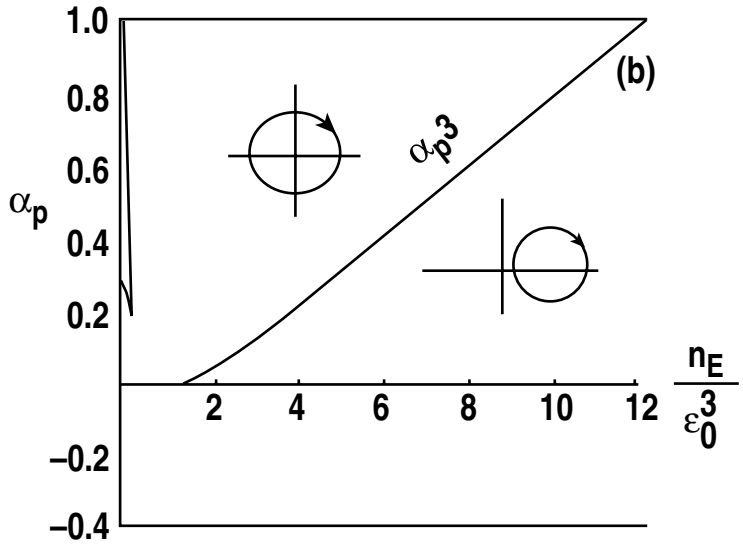

Co-particle start at $\varepsilon_0 = 0.4$, $\theta = 0$; (a) enlarged at lower n_E, (b) at higher n_E

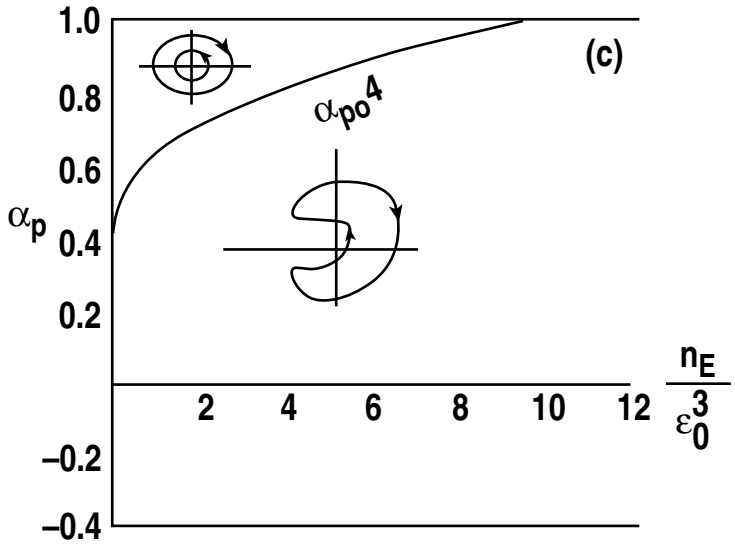

$$\varepsilon^2 = \frac{\psi}{I_a R_1} \qquad \eta_p = \eta_E - \eta_\perp$$

$$\eta_E = \frac{2E}{\Omega_0^2 R_1^2} \qquad \alpha_p = \eta_p / \eta_E$$

$$\eta_\perp = \frac{2\mu B_0}{\Omega_0^2 R_1^2}$$

Counter-particle start at $\varepsilon_0 = 0.4$, $\theta = 0$

MONTE-CARLO ORBITS

- Ion trajectories are calculated by solving the Hamiltonian guiding center (drift) equations [9]:

$$\frac{d}{dt}\left\{P_\varsigma, P_\theta\right\} = -\partial_{\varsigma,\theta} H \quad , \qquad \frac{d}{dt}\left\{\varsigma,\theta\right\} = \partial_{P_\varsigma, P_\theta} H \quad , \tag{1}$$

where

$$P_\theta = I\left(\rho_{||} + \alpha\right) + \Psi \quad , \quad P_\varsigma = g\left(\rho_{||} + \alpha\right) - \Psi_p \quad , \quad H = \frac{1}{2}\rho_{||}^2 B^2 + \mu B + \Phi \tag{2}$$

- The axisymmetric equilibrium field is expressed through its contravariant and covarient forms:

$$B = \nabla\varsigma \times \nabla\Psi_p + q\left(\Psi_p\right)\nabla\Psi_p \times \nabla\theta \quad , \quad B = g\left(\Psi_p\right)\nabla\varsigma + I\left(\Psi_p\right)\nabla\theta + \delta\nabla\Psi_p \tag{3}$$

where the poloidal angle, θ is chosen so that

$$d^3x = J d\Psi_p d\theta d\varsigma \quad , \qquad J = (gq + I)/B^2 \tag{4}$$

MONTE-CARLO RF AND COLLISION OPERATORS

- Each time an ion passes through the ion cyclotron resonance layer $[\omega_{rf} - k_{||} v_{||} = \Omega(B)]$ its perpendicular velocity component undergoes a random change, $\Delta v_{\perp}$. This increment can be readily obtained from the quasi-linear equation governing the rf-induced particle diffusion in velocity space [Chiu (1999)]: $(k_{\perp} = 0, E_{-} = E_{||} = 0)$:

$$\Delta\mu = \Delta\mu_{rf} \pm \sqrt{2\mu\Delta\mu_{rf}} \quad , \qquad \Delta\mu_{rf} = \frac{1}{2}\frac{e_i^2}{m_i B}\left|E_+\right|^2 \tau_{rf}^2 \quad , \tag{5}$$

$$\tau_{rf} = \begin{cases} \tau_{uc} = \left(2\pi/\left|\dot{\Omega}\right|\right)^{1/2} & \text{if } \sqrt{2\tau_{uc}} \le \tau_c \\ \tau_c = 2\pi\, \mathrm{Ai}(\varsigma)\Big/\left|\ddot{\Omega}/2\right|^{1/3}, \quad \varsigma = -\dot{\Omega}^2\Big/\left|2\ddot{\Omega}^2\right|^{2/3} & \text{if } \sqrt{2\tau_{uc}} \ge \tau_c \end{cases} \tag{6}$$

- Pitch angle scattering and slowing-down collisions are modeled with simple operators [Boozer, Kuo-Petravic (1981)]:

$$\Delta\lambda = -\nu_{\perp}\Delta t\lambda \pm \sqrt{\left(1-\lambda^2\right)\nu_{\perp}\Delta t} \quad , \qquad \Delta v = -\nu_{||}\Delta t v \tag{7}$$

NON-SLIP BOUNDARY PLASMA ROTATION

- In a straight cylinder the steady-state equation for the parallel momentum density is:

$$\frac{1}{r}\frac{\partial}{\partial r} r\chi \frac{\partial}{\partial r} n_i M_i v_\varsigma = -F_\varsigma(r) \quad ,$$

Anomalous momentum diffusion:

$$\chi \simeq a^2/6\ \tau_M \quad : \qquad\qquad \tau_M = \tau_E$$

Non-slip boundary condition:

$$v_\varsigma\ (r=a) = 0 \quad ,$$

Zero angular momentum input:

$$\int_0^a F_\varsigma(r)\, r dr = 0$$

CASE 2: STEADY-STATE SIMULATION-THERMALIZED FAST IONS ARE RE-INJECTED INTO THE INITIAL ANNULUS AS MAXWELLIAN PARTICLES

- Initial and final fast ion velocity distributions are approximately the same indicating a good approximation to steady state

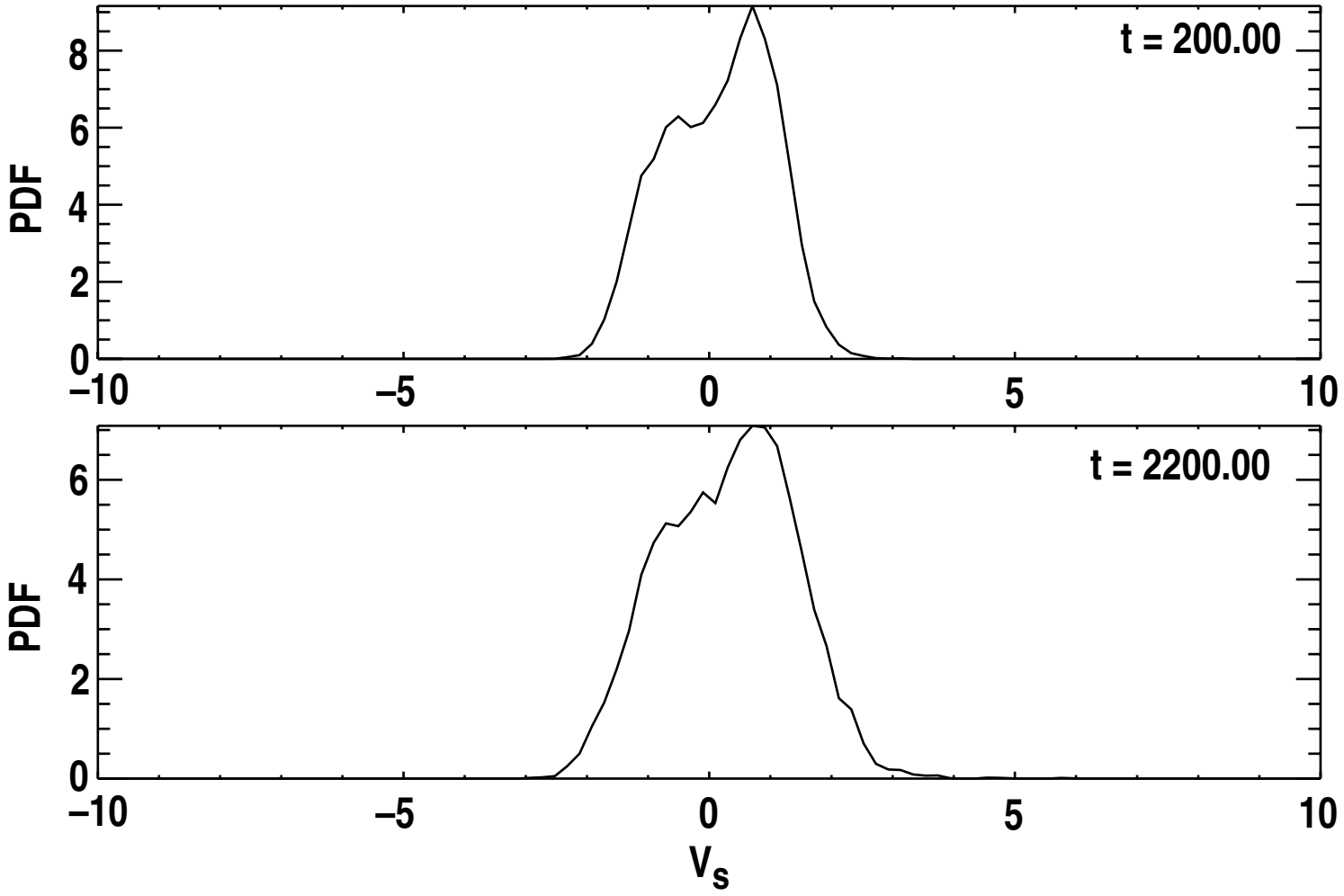

BOTH FAST ION SPATIAL DENSITY DISTRIBUTION AND ICRH ABSORBED POWER DENSITY ALSO REACH STEADY STATE

- Spatial fast ion density peaks around the resonance in a driven system
- Absorbed power density similar to calculation from full-wave code

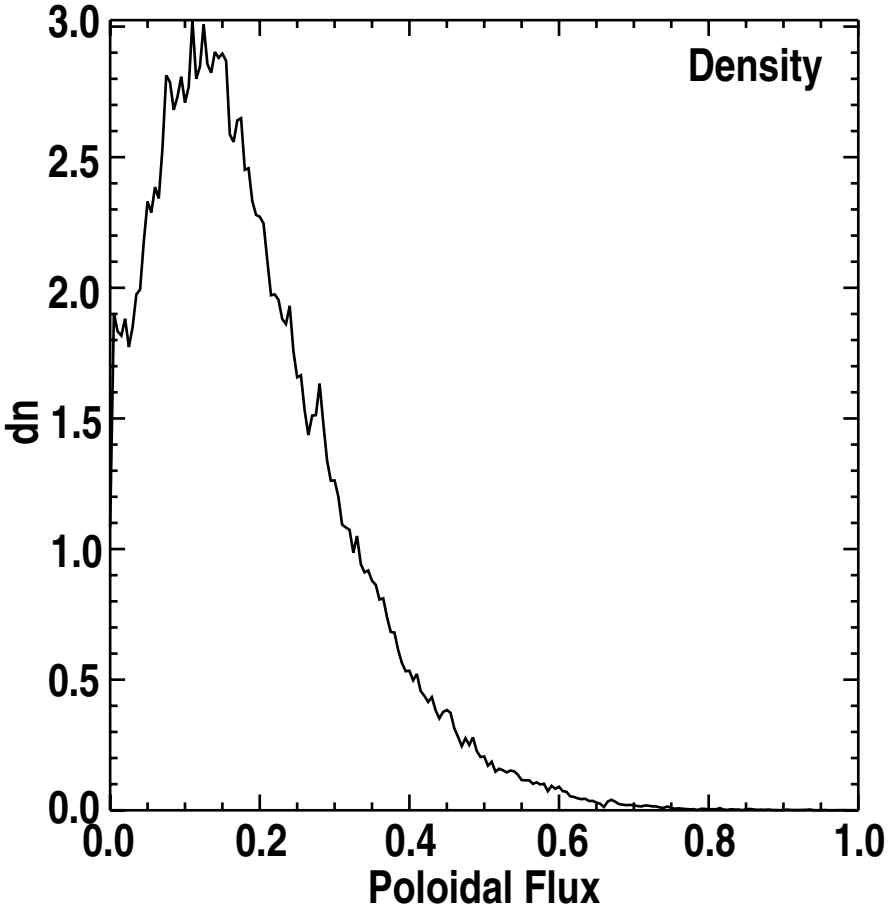

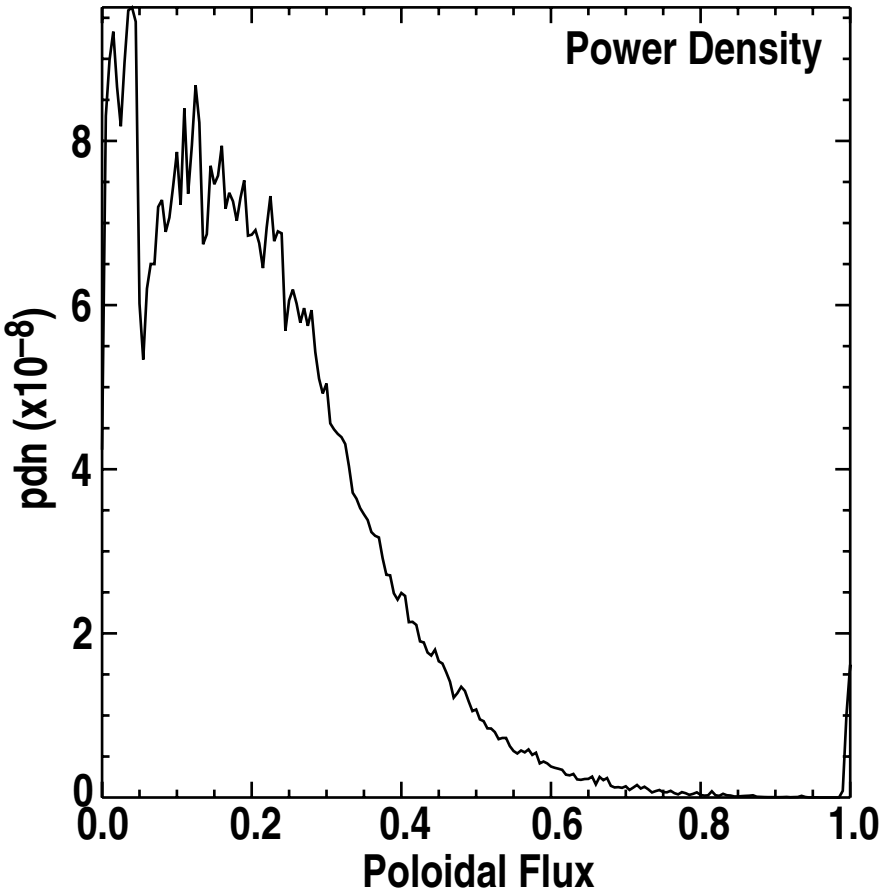

THE STEADY STATE TORQUES SHOW THE SAME FEATURES AS IN THE CASE WITH NO RE-INJECTION

- The magnetic torque shows the ± features from in/out diffusion of fast ions

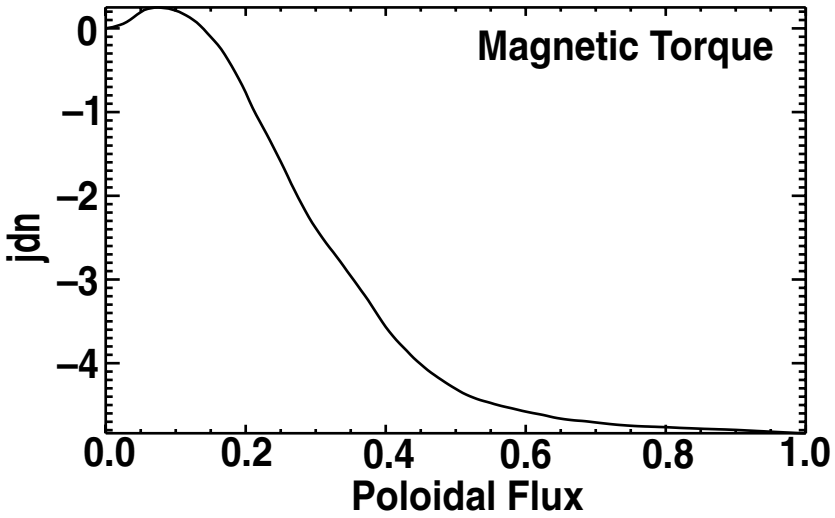

- The frictional torque shows the ± features as explained in Case 1 (HFS)

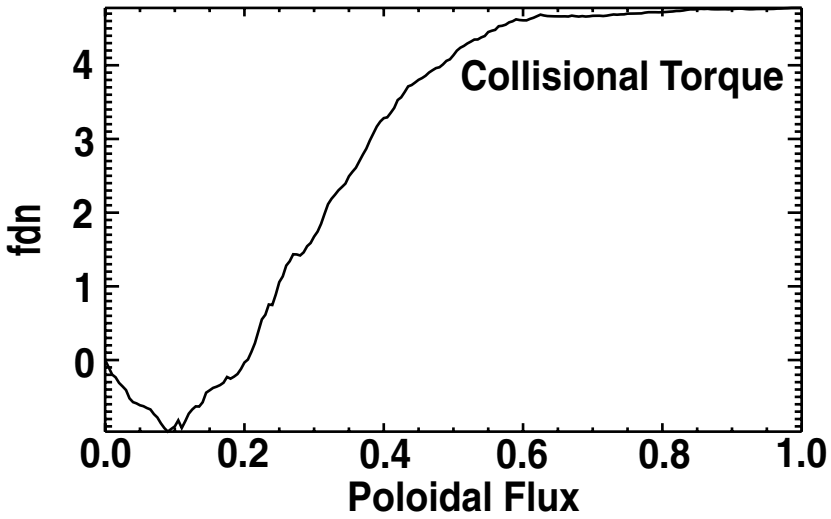

- The net torque is negative resulting in counter-rotation for HFS resonance

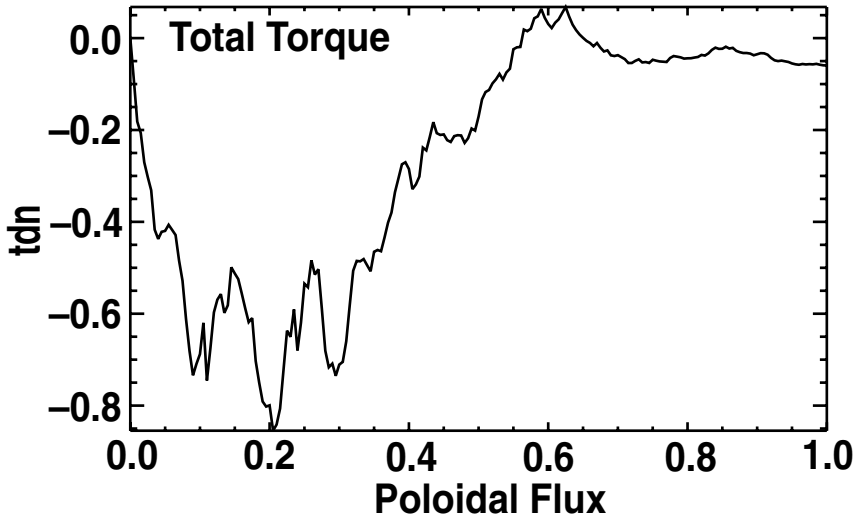

CONCLUSIONS

- **Using a realistic quasi-linear rf operator to self-consistently simulate fast ion heating in a Monte Carlo drift orbit code, we found:**
  - **Co-current rotation with LFS resonance heating**
    - ★ **Due to favorable scattering of "potato" co-passing orbits toward the magnetic axis producing co-frictional torque on bulk**
  - **Counter-current rotation with HFS resonance heating**
    - ★ **Due to favorable detrapping of boundary layer particles into counter-passing particles inside the resonance location leading to counter-frictional torque on bulk**
  - **These features remain in a steady-state rf-driven system**
  - **The co-rotation observed in Alcator C–Mod for HFS resonance remains to be explained. Future studies: higher power, finite $k_{||}$, edge condition**

ORDER OF MAGNITUDE

	DIII–D	C–Mod
R_0	1.65 M	0.67M
a	0.65 M	0.22 M
B	2 T	8 T
q_s	2.1	2.1
R_1	0.39 M	0.16 M
ε_0	0.12 (20 cm)	0.15 (10 cm)
η_{E_c}	5.12×10^{-4}	1.0×10^{-3}
$\rho^2_{E_c}$	0.79 cm^2	0.253 cm^2
E_c (keV)	~15	~78

1. ANALYSIS OF ORBITS NEAR THE AXIS

A Orbits are well described by constants of motion:

$$E = \frac{u_{\|}^2}{2} + \mu B, \qquad \mu = \frac{u_{\perp}^2}{2B}, \qquad P_\zeta = \psi - \frac{I u_{\|}}{\Omega},$$

where

$$(B, \Omega) = \frac{(B_0 \Omega_0)}{1 + \varepsilon \cos\theta}, \qquad I = \pm I_a = R B_T$$

Basic length scale: (δ_ℓ = elongation)

$$R_1 = \frac{\delta_\ell R_0}{2 q_s}$$

Parameters of orbits:

(i) Flux surface parameter (ε = inverse aspect ratio):

$$\varepsilon^2 = \frac{\psi}{I_a R_1}$$

(ii) Invariant energy parameters:

$$\eta_E = \frac{2E}{\Omega_0^2 R_1^2}, \qquad \eta_\perp = \frac{2\mu B_0}{\Omega_0^2 R_1^2}, \qquad \eta_p = \eta_E - \eta_\perp .$$

We can also define pitch angle $\alpha_p = \eta_p / \eta_E$.

(iii) Angular momentum parameters:

$$\eta_\zeta = \frac{P_\zeta}{I_a R_1}$$

Then orbit is well described by

$$\left(\varepsilon^2 - \eta\zeta\right)^2 = \eta_p + \eta_E \varepsilon \cos\theta$$

Alternatively, this can be written as

$$\eta\zeta = \varepsilon^2 - \sigma\sqrt{\eta_p + \eta_E \varepsilon \cos\theta}$$

- η_E, η_p, $\eta\zeta$ and σ completely determines the orbits and thus forms the phase space of orbits

- σ = + 1 is for a co-current moving particle, and σ = –1 is for a counter-current moving particle

- It can be shown that for a given set of η's, a passing co-orbit always encloses a passing counter-orbit

- The orbits of co-and-counter orbits are split, in contrast to thin banana theory, in which they are degenerate in the lowest approximation. This split results in asymmetry in power deposition and subsequent radial excursions

B Analysis of orbits:

On the equatorial plane, the orbit intercepts are given by

$$\left(\varepsilon^2 - \eta\zeta\right)^2 = \eta_p + \eta_E\varepsilon$$

- $\varepsilon > 0$ (<0) represent intercepts at $\theta = 0$ ($= \pi$). Orbit topology is easily deduced graphically

An alternative label for $\eta\zeta$ is intercept at $\theta = 0$, i.e, ε_0

$$\eta\zeta = \varepsilon_0^2 - \sigma\sqrt{\eta_p + \eta_E\varepsilon_0},$$

then

$$\left[\left(\varepsilon^2 - \varepsilon_0^2\right)\left(\varepsilon + \varepsilon_0\right) + 2\sigma\sqrt{\eta_p + \eta_E\varepsilon_0}\left(\varepsilon + \varepsilon_0\right)\right] - \eta_E = 0$$

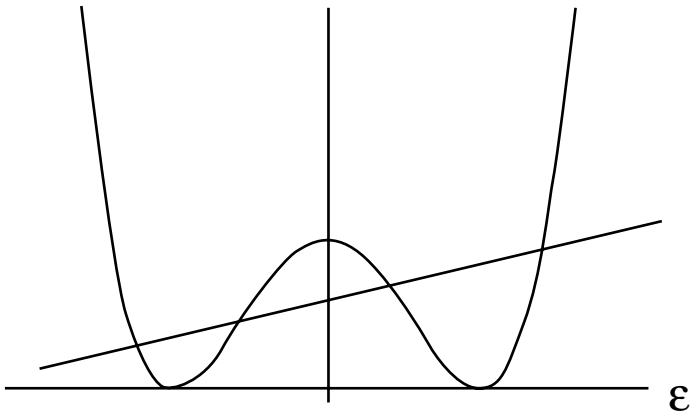

(a) Passing

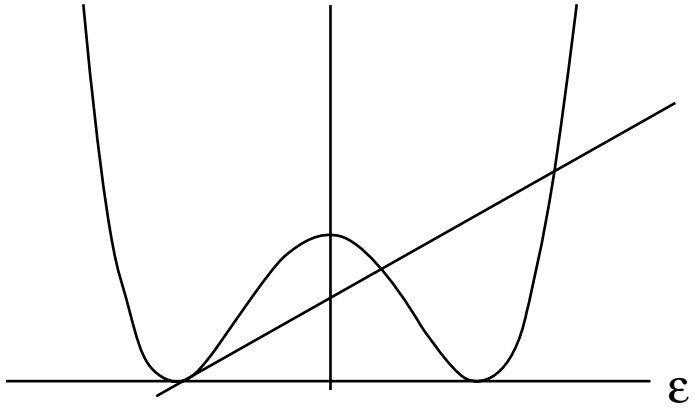

(b) Barely Trapped

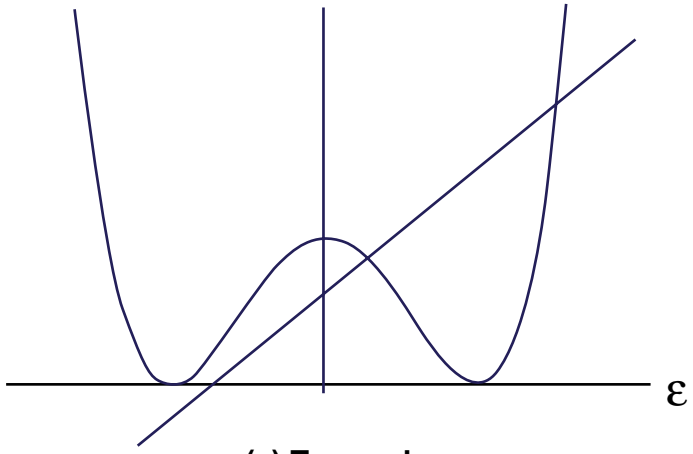

(c) Trapped

(a) σ = + 1 (co-current)

Critical energy $\eta_{EC} = \frac{\delta\varepsilon_0^3}{27}$. There exists two transitions of orbit topologies for $\eta_E < \eta_{EC}$ as a particle pitch angle is increased above the transition values α_{pc2} and α_{pc1}.

$$\alpha_{pc1} = \varepsilon_0\left(\frac{4\varepsilon_0^3\alpha_{Tci}^2}{9\eta_E} - 1\right), \qquad i = 1,2$$

$$\alpha_{Tci} = \frac{1}{4} + \frac{1}{2}\sqrt{2\alpha_E + 1\cos\left[\theta_r - (i-1)\frac{2\pi}{3}\right]}$$

where

$$\theta_r = \frac{1}{3}\tan^{-1}\left(\frac{\sqrt{\alpha_E(4-\alpha_E)^3}}{2 - 10\alpha_E - \alpha_E^2}\right).$$

- For $\alpha_p < \alpha_{pc2}$, particles are trapped. For $\alpha_{pc1} > \alpha_p > \alpha_{pc2}$, a co-passing orbit encloses a counter-passing orbit. For $\alpha_p > \alpha_{pc1}$ only one co-passing orbit exits

- There is a line in the α_p-η_E plane:

$$\alpha_{p3} = \left(\frac{\sqrt{\eta_E}}{2\varepsilon_0} - \frac{\varepsilon_0^2}{2\sqrt{\eta_E}} \right)^2 .$$

For values of η_E greater than those on this line, co-passing particles are confined on the low-field side of the magnetic axis

(b) σ = + 1 (counter-current)

There is only one transition of orbit topologies marking the trapped-passing boundary of co-and-counter particles at $\alpha_p = \alpha_{pc4}$ which is given by

$$\alpha_{pc4} = \varepsilon_0 \left(\frac{4\varepsilon_0^3 \alpha_{Tc4}^2}{9\eta_E} - 1 \right)$$

where

$$\alpha_{Tc4} = \frac{1}{4}\left\{-1+\left[\frac{\alpha_E^2+10\alpha_E-2}{2}+\frac{1}{2}\sqrt{\alpha_E(\alpha_E-4)^3}\right]^{1/3}+\left[\frac{\alpha_E^2+10\alpha_E-2}{2}\right]-\frac{1}{2}\sqrt{\alpha_E(\alpha_E-4)^3}^{1/3}\right\} \quad \text{for } \alpha_E > 4$$

$$= -\frac{1}{4}+\frac{1}{2}\sqrt{2\alpha_E+1}\cos(\theta_{T4}) \quad . \qquad \text{for } \alpha_E > 4$$

$$\theta_{T4} = \frac{1}{3}\tan^{-1}\left(\frac{\sqrt{\alpha_E(4-\alpha_E)^3}}{\alpha_E^2+10\alpha_E-2}\right) \quad .$$

- There is an η_{E4} at which $\alpha_{pc4} = 1$. For $\eta_E > \eta_{E4}$, all counter-particles starting from (θ=0, ε=ε_0) are trapped